Annals of Botany **131**: 323–334, 2023
https://doi.org/10.1093/aob/mcac155, available online at www.academic.oup.com/aob

ANNALS OF BOTANY
Founded 1887

Tree peony PsMYB44 negatively regulates petal blotch distribution by inhibiting dihydroflavonol-4-reductase gene expression

Yuting Luan[1,†], Zijie Chen[1,†], Yuhan Tang[1], Jing Sun[1], Jiasong Meng[1], Jun Tao[1,2,*] and Daqiu Zhao[1,*]

[1]College of Horticulture and Landscape Architecture, Yangzhou University, Yangzhou 225009, China and [2]Joint International Research Laboratory of Agriculture and Agri-Product Safety, the Ministry of Education of China, Yangzhou University, Yangzhou 225009, China
**For correspondence. E-mail dqzhao@yzu.edu.cn or taojun@yzu.edu.cn*
[†]These authors contributed equally to this work.

Received: 7 August 2022 Returned for revision: 4 November 2022 Editorial decision: 12 December 2022 Accepted: 14 December 2022
Electronically published: 19 December 2022

• **Background and Aims** The tree peony (*Paeonia suffruticosa* Andr.) has been widely cultivated as a field plant, and petal blotch is one of its important traits, which not only promotes proliferation but also confers high ornamental value. However, the regulatory network controlling blotch formation remains elusive owing to the functional differences and limited conservation of transcriptional regulators in dicots.
• **Methods** We performed phylogenetic analysis to identify MYB44-like transcription factors in *P. suffruticosa* blotched cultivar 'High noon' petals. A candidate MYB44-like transcription factor, PsMYB44, was analysed via expression pattern analysis, subcellular localization, target gene identification, gene silencing in *P. suffruticosa* petals and heterologous overexpression in tobacco.
• **Key Results** A blotch formation-related MYB44-like transcription factor, PsMYB44, was cloned. The C-terminal of the PsMYB44 amino acid sequence had a complete C2 motif that affects anthocyanin biosynthesis, and PsMYB44 was clustered in the MYB44-like transcriptional repressor branch. PsMYB44 was located in the nucleus, and its spatial and temporal expression patterns were negatively correlated with blotch formation. Furthermore, a yeast one-hybrid assay showed that PsMYB44 could target the promoter of the late anthocyanin biosynthesis-related dihydroflavonol-4-reductase (*DFR*) gene, and a dual-luciferase assay demonstrated that PsMYB44 could repress *PsDFR* promoter activity. On the one hand, overexpression of *PsMYB44* significantly faded the red colour of tobacco flowers and decreased the anthocyanin content by 42.3 % by downregulating the expression level of the tobacco *NtDFR* gene. On the other hand, *PsMYB44*-silenced *P. suffruticosa* petals had a redder blotch colour, which was attributed to the fact that silencing *PsMYB44* redirected metabolic flux to the anthocyanin biosynthesis branch, thereby promoting more anthocyanin accumulation in the petal base.
• **Conclusion** These results demonstrated that PsMYB44 negatively regulated the biosynthesis of anthocyanin by directly binding to the *PsDFR* promoter and subsequently inhibiting blotch formation, which helped to elucidate the molecular regulatory network of anthocyanin-mediated blotch formation in plants.

Key words: anthocyanin biosynthesis, MYB44-like transcription factor, transcriptional repressor, dihydroflavonol-4-reductase, blotch formation, tree peony.

INTRODUCTION

In ornamental plants, carotenoids, anthocyanins and betaines endow plants with vivid colours to differentiate them from green (Tanaka *et al.*, 2008; Miller *et al.*, 2011), among which anthocyanin is a particularly important component. Anthocyanin is a rich secondary metabolite and exists widely in plant organs such as leaves, flowers and fruits (Wang *et al.*, 2019*b*; Li *et al.*, 2021*b*, 2021*c*). Anthocyanin has various biological functions, including ultraviolet protection, disease resistance, response to abiotic stress and potential benefits to human health (Albert *et al.*, 2018; Li *et al.*, 2020, 2022). In addition, anthocyanin affects the appearance of ornamental plants, which might increase the number of visits by pollinators such as moths or bees and improve reproductive diversity in insect-dependent flowering plants (Moeller 2005; Eckhart *et al.*, 2006).

In the past few decades, the anthocyanin biosynthesis pathway in plants has been reported comprehensively, and its metabolism has been well characterized and considered to be relatively conserved, especially in land plants (Glover *et al.*, 2013; Tohge *et al.*, 2013, 2017). According to previous studies, there are two types of genes, early biosynthetic genes (EBGs) and late biosynthetic genes (LBGs), which are responsible for hierarchical anthocyanin biosynthesis. The EBGs include genes encoding chalcone synthase (CHS), chalcone isomerase (CHI), flavanone 3-hydroxylase (F3H) and flavonol synthase (FLS), which are located upstream of flavonoid metabolism, usually provide precursor substrates of dihydrokaempferol and dihydroqueretin and are responsible for the biosynthesis

of flavonol, anthocyanin and proanthocyanidin (PA) (Rausher *et al.*, 1999). In contrast, LBGs, including genes encoding dihydroflavonol 4-reductase (DFR), anthocyanidin synthase (ANS) and flavonoid *O*-methyltransferase (FOMT), are specifically responsible for the biosynthesis and modification of anthocyanin (Holton and Cornish, 1995). To date, numerous regulatory genes affecting plant anthocyanin biosynthesis and their regulatory mechanisms have been revealed in different species. For instance, several EBGs in the dicot model plant *Arabidopsis* are generally regulated by R2R3-MYB regulators AtMYB11, AtMYB12 and AtMYB111, which help to absorb ultraviolet rays (Stracke *et al.*, 2007). A ternary complex represented by *Arabidopsis* AtPAP1, AtTT8 and AtTTG1 activates anthocyanin metabolic flux by regulating the expression of LBGs (Hichri *et al.*, 2011). In the monocot plant *Zea mays*, both EBGs and LBGs are regulated by the MYB-bHLH-WD40 (MBW) ternary complex (Petroni and Tonelli, 2011). To date, this hierarchical regulatory mechanism has been well characterized in horticultural plants, including *F.* × *ananassa*, *Actinidia chinensis*, *Petunia hybrida* and *Malus domestica* (Yamagishi *et al.*, 2010; Schaart *et al.*, 2013; An *et al.*, 2019; Wang *et al.*, 2019*a*). This network is always under the common transcriptional regulation, with MYB regulators at the core. However, regulatory genes in plants always evolve much faster than structural genes (Rausher *et al.*, 1999; Sheehan *et al.*, 2016; Huang *et al.*, 2018), thus their regulatory mechanisms in different species are less restricted and need to be further explored.

In addition to MYB activators, the coloration of many horticultural plant organs is influenced by feedback mechanisms mediated by anthocyanin-related MYB repressors, and the spatial and temporal changes in this phenomenon might be attributed to the homeostatic balance of plant growth. For instance, *M. domestica* MdMYB306 fine-tunes peel anthocyanin accumulation as a result of its inhibition of anthocyanin overaccumulation activated by *MdDFR* gene and MdMYB17 activator (Wang *et al.*, 2022). In *Prunus persica*, the typical R2R3-MYB repressor PpMYB18 is a competitor of PpMYB10.1 activator, preventing excessive accumulation of PAs and anthocyanins during fruit ripening (Hui *et al.*, 2019). To date, several novel MYB44-like repressors have been characterized in *Solanum tuberosum* and *Ipomoea batatas* (Liu *et al.*, 2019; Li *et al.*, 2021*a*). However, this type of regulatory mechanism specialized in a limited pathway of different plants, such as *Pyrus bretschneideri* PbMYB120 for *PbUFGT1*, grape hyacinth MaMYBx for competition with MabHLH1, and *Narcissus tazetta* NtMYB3 for *NtFLS* (Anwar *et al.*, 2019; Song *et al.*, 2020; Zhang *et al.*, 2020*a*). Overall, the balance mechanism of anthocyanins in dicotyledonous plants is far more complex than that in monocotyledonous plants, given that a large variability has been elucidated among different cultivars, such as in *Chrysanthemum morifolium*, *M. domestica* and *Paeonia* (Du *et al.*, 2015; Meng *et al.*, 2016; Xiang *et al.*, 2019).

The tree peony (*Paeonia suffruticosa* Andr.) is a traditional flower native to China that is famous for its colourful flowers and rich oil production. Previous studies have shown that different *P. suffruticosa* cultivars accumulate abundant flavonoid compounds, including anthocyanins that contribute to their red colours and anthoxanthins that contribute to their yellow or white colour (Li *et al.*, 2009). More deeply, the flower colour regulation system in *P. suffruticosa* has been revealed in different cultivars and shown to be relatively conservative compared with model plants. Several anthocyanin activators, including PsMYB58, PsMYB57, PsMYB114L and PsMYB12L, were isolated from *P. suffruticosa* flowers and shown to have positive functions in anthocyanin accumulation (Zhang *et al.*, 2019, 2020*b*, 2021). Moreover, some more explicit models of hierarchical regulation, such as specific spatial and temporal regulation models of PsbHLH1 for *PsDFR* and *PsANS* or the PsMYB12-bHLH-WD40 complex for *PsCHS*, have also been reported in red and blotched *P. suffruticosa* petals (Gu *et al.*, 2018; Qi *et al.*, 2020). However, in comparison to other species, MYBs are still rarely isolated from *P. suffruticosa*, which is a constraining factor limiting the study of *P. suffruticosa* flower colour, and reports on the anthocyanin repressors are lacking.

In this study, *P. suffruticosa* cultivar 'High noon', which shows a specific blotch rendering pattern, was investigated for analysis of anthocyanin accumulation. Next, a MYB regulatory gene, *PsMYB44*, was isolated from *P. suffruticosa*, and its spatial and temporal expression was revealed in 'High noon' petals. Furthermore, a yeast one-hybrid (Y1H) assay and dual-luciferase assay were applied to find the potential target genes of PsMYB44, and its function was validated by introducing *PsMYB44* into tobacco and *P. suffruticosa* petals. These results lay the foundations for further clarification of the underlying mechanism of spatial blotch distribution in *P. suffruticosa.*

MATERIALS AND METHODS

Plant materials and growth conditions

Paeonia suffruticosa cultivar 'High noon', which has a red blotch at the petal base, *Nicotiana tabacum* cultivar 'k326' and *Nicotiana benthamiana* leaves were used as plant materials for the present study. The non-blotch area and blotch area of *P. suffruticosa* petals at different developmental stages spanning April–May (S1, pigmented stage; S2, unfolded-petal stage; S3, initial-flowering stage; and S4, full-flowering stage) were collected and stored at −80 °C and were prepared for gene and promoter cloning and gene expression analysis. Petals at S1 were used for the virus-induced gene silencing (VIGS) assay. *N. tabacum* and *N. benthamiana* were grown in a greenhouse (25 °C for 16 h light–22 °C for 8 h dark), which were used for stable transformation of key genes and transient assays of key genes and promoters.

DNA and RNA extraction and complementary DNA synthesis

Genomic DNA and total RNA were extracted from different plant samples of *P. suffruticosa* and tobacco using a NuClean Plant Genomic DNA Kit (CWBIO, China) and a MiniBEST Plant RNA Extraction Kit (TaKaRa, Japan), referring to the respective manufacturer's instructions. The quality control of RNA purity and concentration were then assessed by NanoDrop1000 spectrophotometry (Thermo Scientific, USA). Complementary DNA (cDNA) was synthesized from 1000 ng of total RNA with a SMARTer PCR cDNA Synthesis Kit (Clontech, USA).

Gene and promoter cloning, sequence alignment and phylogenetic analysis

To isolate candidate anthocyanin-related transcription factors [*PsMYB44* (cluster_20336); *PsbHLH1* (cluster_44047); *PsbHLH2* (cluster_36427); and *PsbHLH3* (cluster_24228)], PCR amplification of candidate genes was conducted using specific primers (Supplementary Data Table S1) designed by Primer 5.0 based on the *P. suffruticosa* 'High noon' full-length transcriptome database of one mixed petal sample from S1–S4 (National Center for Biotechnology Information sequence read archive accession number: SRP378683; Luan *et al.*, 2022). To isolate promoters of *P. suffruticosa* candidate anthocyanin biosynthetic genes, PCR amplification was conducted using specific primers (Supplementary Data Table S1) designed by Primer 5.0, referring to the *P. suffruticosa* genome database (Lv *et al.*, 2019). All PCR products with predicted lengths were purified and cloned into 5 × TA/Blunt-Zero Cloning Mix vector (Vazyme, China) for sequence confirmation. The sequences upstream of the ATG start codon were defined as promoters, and the PlantCARE database (http://bioinformatics.psb.ugent.be/webtools/plantcare/html/) was used to find potential MYB-binding sites.

Multiple alignments of *PsMYB44* from *P. suffruticosa* and six MYB repressors from other plants were conducted by DNAMAN 6.0. The conserved domains were highlighted with different colours. For phylogenetic analysis, the amino acid sequences of PsMYB44 from *P. suffruticosa* and 24 anthocyanin-related MYB transcription factors were aligned by the ClustalW, then subjected to MEGA 7.0 to generate a neighbour-joining tree.

Quantitative real-time PCR analysis

P. suffruticosa spatial (non-blotch and blotch) and temporal (from S1 to S4) petals, treated petals and *N. tabacum* petals were used to study the gene expression patterns. Total RNA of different samples was extracted as above, and HiScript QRT SuperMix for qPCR (Vazyme, China) was used for first-strand cDNA synthesis. Transcription expression levels were analysed using NovoStart SYBR qPCR Super Mix (Novoprotein, China) by a BIO-RAD CFX Connect Optics Module (Bio-Rad, USA). The details of the PCR parameters were described in a previous study (Zhao *et al.*, 2020). Transcript abundance data were normalized using *P. suffruticosa β-Tubulin* (EF608942) and *N. tabacum Actin* (AB158612) internal controls, respectively. The relative expression levels of the candidate genes were calculated according to the $2^{-\Delta\Delta Ct}$ method. All primers used are listed in Supplementary Data Table S2.

Subcellular localization

For subcellular localization, the coding sequence (CDS) of *PsMYB44* was amplified by PCR technology with specific primers (forward, 5′-CGGGGATCCTCTAGAGTCGACATGTCAATTTCGAGGAAAGATATGAA-3′; reverse, 5′-CACCATGGTACTAGTGTCGACCTCAGCCTTGCTAATTGCCATA-3′) and fused into the *p35S:GFP* vector encoding a green fluorescent protein (GFP) (Supplementary Data Fig. S1). Subsequently, the fusion construct (*p35S:PsMYB44-GFP* vector), empty *p35S:GFP* vector and mCherry protein directed to the nucleus localization signal (NLS) were transformed into *Agrobacterium tumefaciens* strain GV3101 by a freeze–thaw method (Shaner *et al.*, 2004). Approximately 4- to 5-week-old *N. benthamiana* leaves were used as receptor materials, and the GFP and red fluorescent protein (RFP) signals were observed at 488 and 561 nm by confocal laser microscopy (Nikon C2-ER, Japan) to determine the subcellular localization of PsMYB44.

Yeast one-hybrid and yeast two-hybrid assays

For the Y1H assay, the CDS of *PsMYB44* was amplified with specific primers and cloned upstream of the GAL4-activation domain of the pGADT7 vector as prey plasmids. The putative promoters of *PsCHS* (1764 bp), *PsCHI1* (716 bp), *PsF3H1* (1716 bp), *PsDFR* (2052 bp) and *PsANS* (1256 bp) genes were cloned into the pAbAi vector as a promoter of the aureobasidin A resistance (*AurR*) gene as bait plasmids (Supplementary Data Fig. S2). Selection of the minimal inhibitory concentration of these promoters was performed as previously described (Luan *et al.*, 2022). Subsequently, the pGADT7-*PsMYB44* vector was introduced for interaction analysis on SD/-Leu medium with Aureobasidin A (AbA), and the interaction relationships were determined by the growth conditions of yeast cells.

For the yeast two-hybrid (Y2H) assay, the CDSs of *PsbHLH1-3* were amplified with specific primers and cloned upstream of the GAL4-binding domain of pGBKT7 vector as bait plasmids, and the above fusion pGADT7-*PsMYB44* vector was used as the prey plasmid (Supplementary Data Fig. S3). The different combinations containing bait and prey plasmids were cotransformed in Y2H Gold strain yeasts (Clontech, USA). Subsequently, the positive yeast cells were selected on SD double-dropout (DDO) medium, SD triple-dropout (TDO) medium and SD quadruple-dropout (QDO) medium with AbA. After 3–5 days of cultivation at 30 °C, the presence of interaction relationships between PsMYB44 and PsbHLH1-3 was determined by the growth conditions of the yeast cells. All primers used are listed in Supplementary Data Tables S3 and S4.

Dual-luciferase assay

Dual-luciferase assays were performed in *N. benthamiana* leaves as previously reported (Hellens *et al.*, 2005). The promoter of the *PsDFR* gene was cloned into pGreenII 0800 5-LUC vector as a reporter plasmid, and the CDS of *PsMYB44* was cloned into pGreenII 0029 62-SK vector as an effector plasmid. The fusion constructs and empty effector were transformed individually into *A. tumefaciens* strain GV3101 as above. *Agrobacterium* cultures containing PsMYB44 and empty SK vector were mixed with *PsDFR* promoter at a ratio of 10:1 to infiltrate 4- to 5-week-old *N. benthamiana* leaves. After 2 days of weak light cultivation, firefly luciferase (LUC) and *Renilla* luciferase (REN) activities were measured with a Dual-Luciferase Reporter Assay Kit (Vazyme, China), and the LUC/REN ratio was used to determine the regulatory effect of PsMYB44 on *PsDFR* promoter. All primers used are listed in Supplementary Data Table S5.

Stable transformation in tobacco

The CDS of *PsMYB44* was cloned into pCAMBIA1301 vector as overexpression plasmids (Supplementary Data Fig. S4). Then, *PsMYB44* was stably overexpressed in tobacco 'k326' using the leaf disc method (Sunilkumar *et al.*, 1999). The T2 transgenic plants were first validated by PCR and qRT-PCR, and the changes in flower phenotype were observed between wild-type (WT) and transgenic lines at the full-flowering stage. Furthermore, determination of the colour index and measurement of anthocyanin accumulation and detection of the anthocyanin biosynthetic gene expression level were performed to investigate the underlying reason for changes in flower colour. All primers used are listed in Supplementary Data Tables S2 and S6.

Virus-induced gene silencing assay

Virus-induced *PsMYB44* silencing was performed based on a tobacco rattle virus (TRV)-based VIGS system generating pTRV1 and pTRV2 (Supplementary Data Fig. S5) (Liu *et al.*, 2002). The fusion constructs (TRV2-*PsMYB44* vector), empty TRV2 vector and TRV1 vector were individually transformed into *A. tumefaciens* strain GV3101 as above. *Agrobacterium* cultures containing *PsMYB44*, TRV2 and TRV1 were mixed at a ratio of 1:1 to infiltrate *P. suffruticosa* petals at S1. After washing twice with sterile water, petals were cultured on the ½ Murashige and Skoog (MS) medium. Phenotypic observation, determination of the colour index, measurement of flavonoid accumulation and detection of the anthocyanin biosynthetic gene expression level were performed on WT and *PsMYB44*-silenced petals at 7 days. All primers used are listed in Supplementary Data Tables S2 and S7.

Measurement of anthocyanins and anthoxanthins

Total anthocyanins and anthoxanthins were determined in both *P. suffruticosa* and *N. tabacum* petals using high-performance liquid chromatography (HPLC) as previously described (Zhao *et al.*, 2015). Briefly, 0.2 g of fresh flower powders were soaked in 1.2 mL of methanol solution (containing 0.1 % HCl) and shaken at 4 °C overnight in the dark. Then, the extract was used for qualitative and quantitative analysis of flavonoids using an LCQ Deca XP MAX liquid chromatography–mass spectrometry (HPLC-ESI-MSn) Agilent 1200-6460 HPLC system (Agilent Technologies, Santa Clara, CA, USA). The contents of anthocyanin and anthoxanthin components were assessed semi-quantitatively against cyanidin-3-*O*-glucoside and rutin standards, respectively. The specific details can be found in the study by Luan *et al.* (2022).

Statistical analysis

The variance of the results was analysed with the SAS/STAT statistical analysis package (v.6.12, SAS Institute, Cary, NC, USA). Means were considered statistically significant at $P < 0.05$.

RESULTS

Isolation and characterization of PsMYB44

Plant MYB44-like transcription factors have been validated as flavonoid-related transcriptional repressors in many plants (Gao *et al.*, 2011; Liu *et al.*, 2019; Meng *et al.*, 2022). Initially, basic local alignment search tool (BLAST) was used to search for PsMYB44-like transcription factors in *P. suffruticosa* transcriptome data. Subsequently, one sequence was found and initially named *PsMYB44* for further functional determination. *PsMYB44*, comprising a 987 bp coding sequence, encoded 328 amino acid residues. PsMYB44 protein was in alignment with typical R2R3-MYB repressors, including *Arabidopsis thaliana* AtMYB4 protein, *F.* × *ananassa* FaMYB1 protein and other known MYB44-like proteins in other plants. As shown in Fig. 1A, PsMYB44 possessed a typical complete R2R3 domain, ranging from 12 to 109, for binding to DNA sequences. Moreover, only AtMYB4 contained a C1 motif in the C-terminal, whereas other sequences seemed to gap this feature. In addition to the C1 motif, another repressor-characterized C2 motif was found in all of these sequences, including PsMYB44, which might be the key motif for their repressive functions.

To define the affinity of PsMYB44, a phylogenetic analysis of 25 plant R2R3-MYB proteins associated with various functions in flavonoid biosynthesis was performed. It was found that PsMYB44 belonged to the MYB44-like repressor class independent of anthocyanin-related activators and repressors, and 79 % homology was detected between PsMYB44 and *S. tuberosum* StMYB44-1 (Liu *et al.*, 2019), which indicated that *PsMYB44* might be involved in anthocyanin biosynthesis (Fig. 1B).

PsMYB44 is negatively correlated with blotch formation

In our previous study, we found that anthocyanin accumulation levels increased with petal development, peaked at S2 in blotch areas, then decreased at S3 and S4, while no anthocyanin accumulated in non-blotch areas (Luan *et al.*, 2022). To explore the relationship between *PsMYB44* expression levels and the blotch formation and distribution in *P. suffruticosa* petals, qRT-PCR analysis was performed and showed that *PsMYB44* expression levels in non-blotch areas were always higher than those in blotch areas, which was generally opposite to the spatial distribution of blotch. Notably, the expression levels of *PsMYB44* increased gradually with petal development (Fig. 2). These results suggested that *PsMYB44* might play a negative role in anthocyanin biosynthesis in *P. suffruticosa*. For further study of *PsMYB44* functions, the *PsMYB44* GFP fusion construct was used to detect the subcellular localization of PsMYB44, and *PsMYB44* GFP fusion protein signals were fully fused with NLS-RFP signals in the *N. benthamiana* leaves, indicating that PsMYB44 was located in the nucleus (Fig. 3).

PsMYB44 is an anthocyanin repressor that inhibits PsDFR expression

To test the effects of PsMYB44 on the transcription levels of anthocyanin biosynthetic genes, the promoters of five

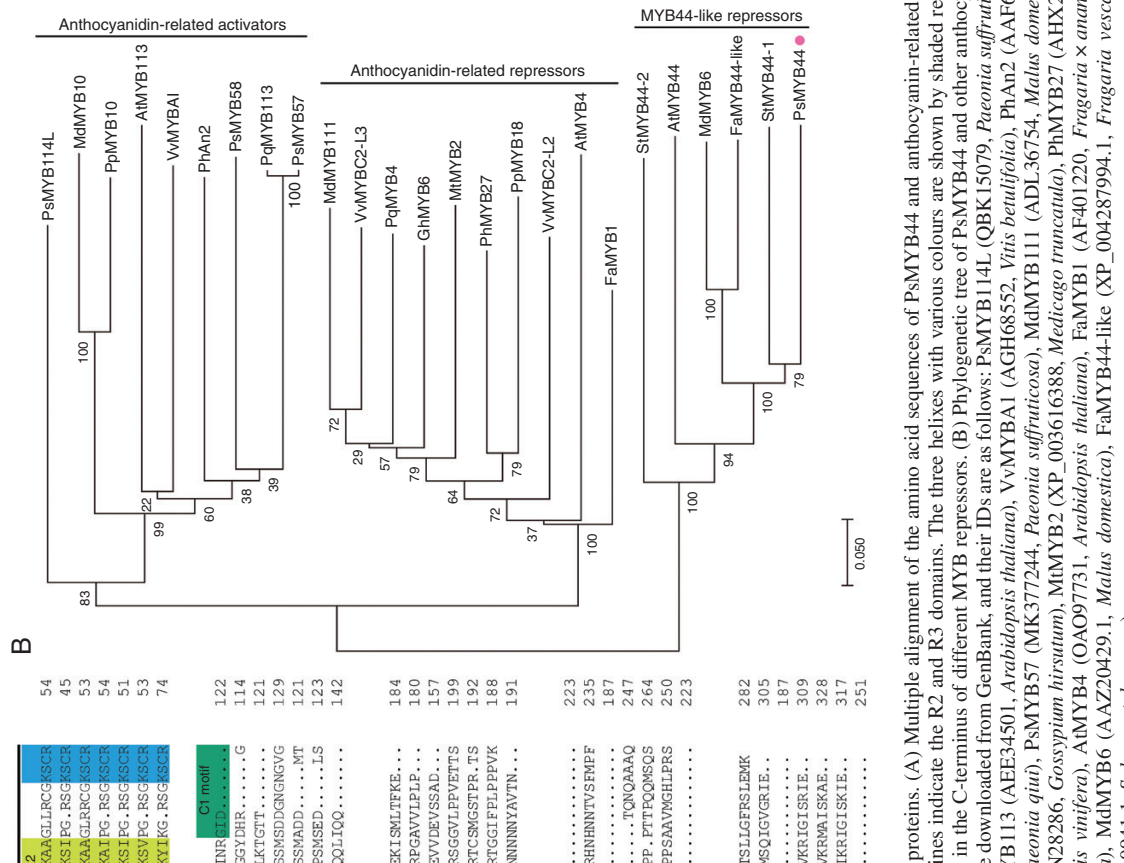

FIG. 1. Amino acid sequence alignment and phylogenetic analysis of PsMYB44 and other MYB proteins. (A) Multiple alignment of the amino acid sequences of PsMYB44 and anthocyanin-related MYB repressor proteins. PsMYB44 isolated from *Paeonia suffruticosa* is marked with a red dot. Overlines indicate the R2 and R3 domains. The three helixes with various colours are shown by shaded residues in the R2 and R3 domains, respectively. Distinct colours indicate the conserved C1 and C2 motifs in the C-terminus of different MYB repressors. (B) Phylogenetic tree of PsMYB44 and other anthocyanin-related MYB proteins in other plants. PsMYB44 is indicated with a red dot. Protein sequences were downloaded from GenBank, and their IDs are as follows: PsMYB114L (QBK15079, *Paeonia suffruticosa*), MdMYB10 (ABB84753.1, *Malus domestica*), PpMYB10 (ADK73605.1, *Prunus persica*), AtMYB113 (AEE34501, *Arabidopsis thaliana*), VvMYBA1 (AGH68552, *Vitis betulifolia*), PhAn2 (AAF66727, *Petunia* × *hybrida*), PsMYB58 (MW429211, *Paeonia suffruticosa*), PqMYB113 (QCF29938, *Paeonia qiui*), PsMYB57 (MK377244, *Paeonia suffruticosa*), MdMYB111 (ADL36754, *Malus domestica*), VvMYBC2-L3 (AIP98385, *Vitis vinifera*), PqMYB4 (QCF29939, *Paeonia qiui*), GhMYB6 (AAN28286, *Gossypium hirsutum*), MtMYB2 (XP_003616388, *Medicago truncatula*), PhMYB27 (AHX24372, *Petunia* × *hybrida*), PpMYB18 (ALO81021, *Prunus persica*), VvMYBC2-L2 (ACX50288, *Vitis vinifera*), AtMYB4 (OAO97731, *Arabidopsis thaliana*), FaMYB1 (AF401220, *Fragaria* × *ananassa*), StMYB44-2 (MK410942.1, *Solanum tuberosum*), AtMYB44 (AF339698, *Arabidopsis thaliana*), MdMYB6 (AAZ20429.1, *Malus domestica*), FaMYB44-like (XP_004287994.1, *Fragaria vesca*) and StMYB44-1 (MK410941.1, *Solanum tuberosum*).

anthocyanin biosynthesis-related candidate structural genes from *P. suffruticosa* were obtained, and these sequences were predicted to contain three, three, two, four and two MYB-binding sites. Next, these promoters were applied to the Y1H assay for detection of interactions. As shown in Fig. 4A, PsMYB44 could bind to the promoter of *PsDFR*, because the transgenic yeast cells could grow normally on the AbA-containing medium, which meant that PsMYB44 might influence the transcription level of *PsDFR*. To confirm the capability of PsMYB44 to inhibit *PsDFR* transcription levels, the *P. suffruticosa PsDFR* promoter was fused upstream of the LUC reporter gene. As shown in Fig. 4B, infiltration of PsMYB44 greatly reduced the LUC/REN value by 60.0 % when compared with the empty vector, which suggested that PsMYB44 was a negative regulator of anthocyanin biosynthesis in *P. suffruticosa* petals.

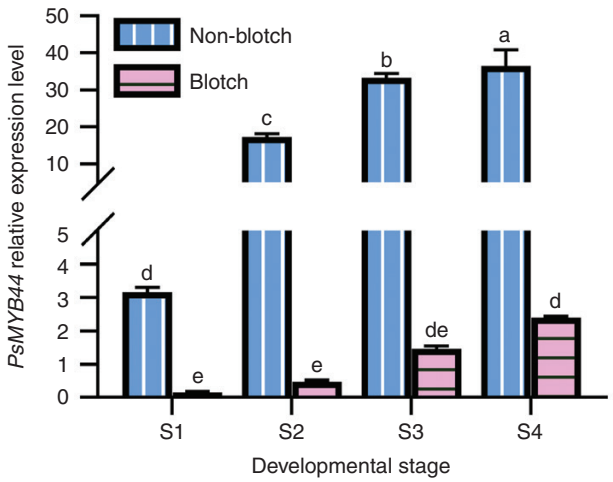

FIG. 2. Analysis of the expression pattern of *PsMYB44* in *Paeonia suffruticosa* non-blotch and blotch areas from S1 to S4 detected by qRT-PCR. Abbreviations: S1, pigmented stage; S2, unfolded-petal stage; S3, initial-flowering stage; and S4, full-flowering stage. The values are shown as the mean + SD, and different letters indicate significant differences ($P < 0.05$).

PsMYB44 is a PsbHLH1-3 independent repressor

According to a previous study in other plants, negative R2R3-MYB anthocyanin regulators either compete with bHLH cofactors or form inhibitory complexes to inhibit anthocyanin biosynthesis (Wang *et al.*, 2019*a*, 2022; Ni *et al.*, 2021). In the present study, Y2H assays were performed to investigate whether the inhibitory function of PsMYB44 was dependent on PsbHLH cofactors. The pGBKT7-*PsMYB44* and pGADT7-*PsbHLH1-3* recombination vectors were constructed and transformed into Y2H Gold strain yeasts. The transgenic yeast cells were screened on auxotrophic mediums. As shown in Supplementary Data Fig. S6, PsMYB44 did not interact with PsbHLH1-3.

PsMYB44 negatively regulates anthocyanin accumulation in transgenic tobacco

The function of *PsMYB44* was confirmed via stable transformation in tobacco. After introducing the pCAMBIA1301-*PsMYB44* overexpression construct into tobacco, positive tobacco plants were obtained, and T2 plants were used for subsequent experiments. The flower colour of three *PsMYB44* transgenic lines at the full-flowering stage was much lighter than that of WT (Fig. 5A). PCR and qRT-PCR were used to analyse the presence and expression level of *PsMYB44*, and *PsMYB44* was strongly expressed in three transgenic plants,

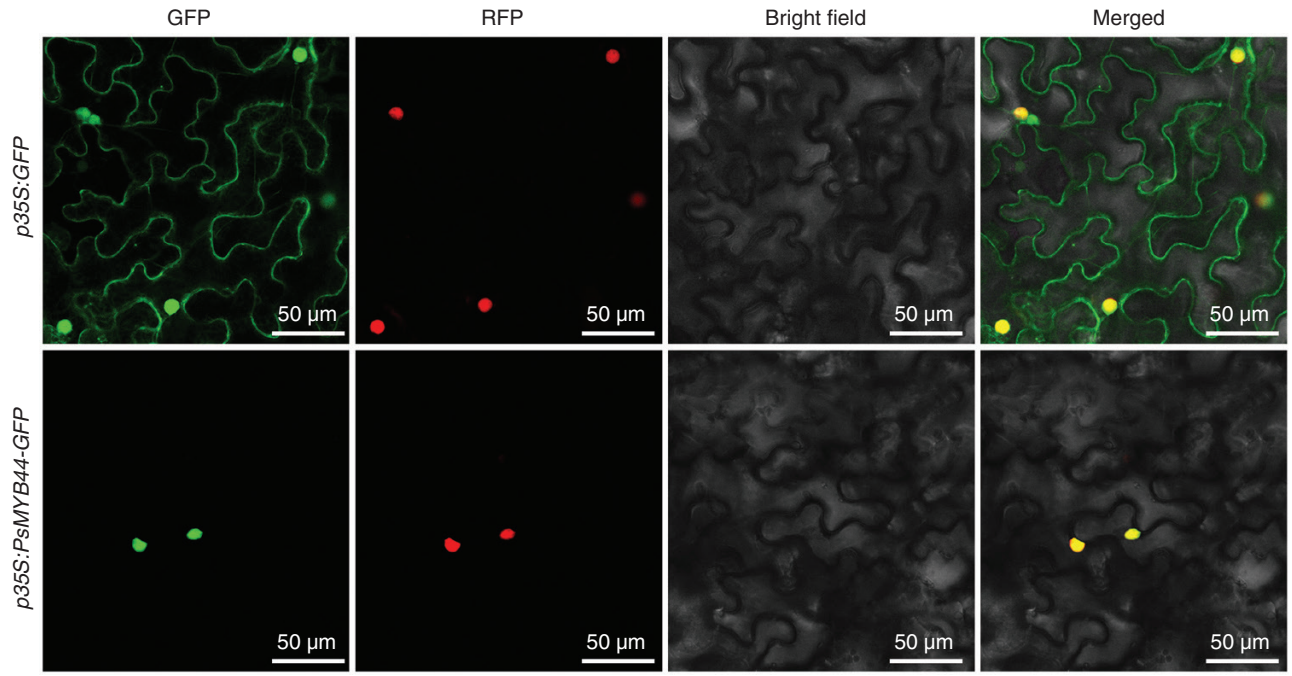

FIG. 3. Subcellular localization of PsMYB44 in tobacco leaves. The red fluorescent signals represent localization in the nucleus driven by red fluorescent protein.

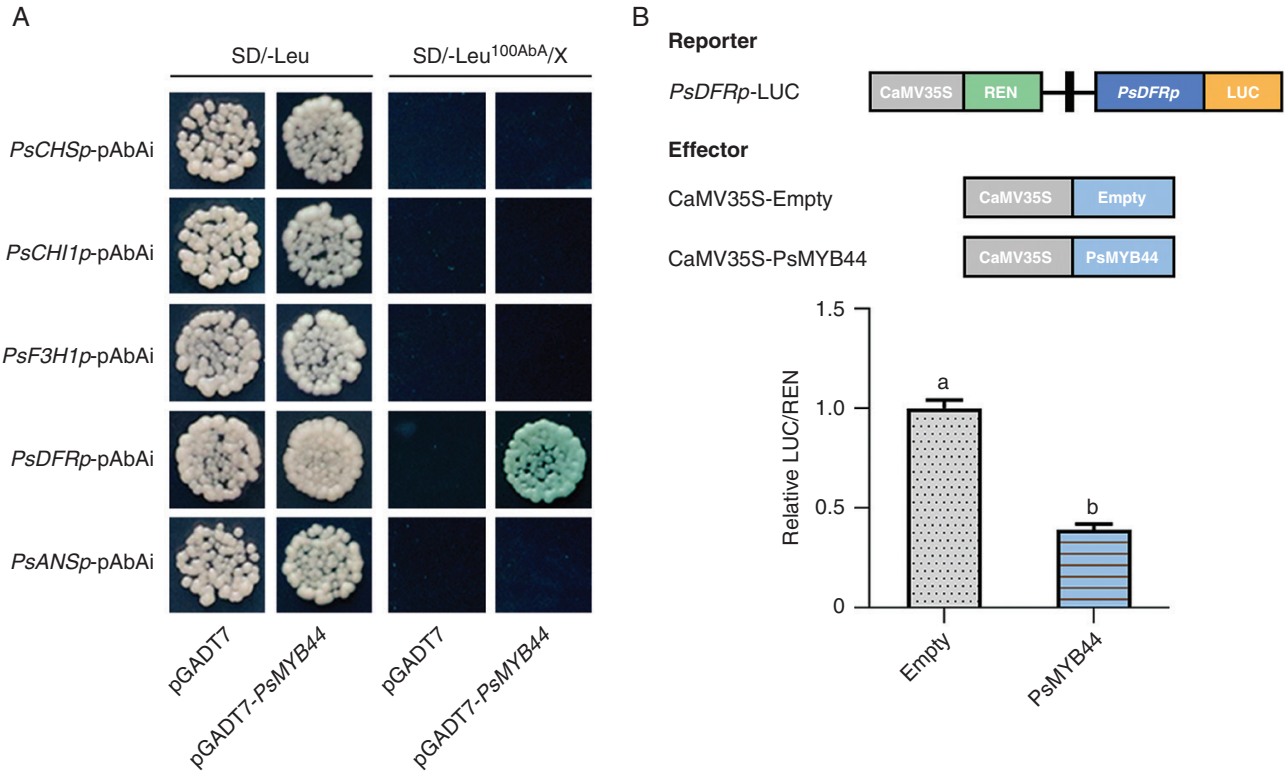

FIG. 4. PsMYB44 binds to *PsDFR* promoter and inhibits its transcription. (A) A yeast one-hybrid assay for analysis of the interaction between PsMYB44 and anthocyanin biosynthetic genes in *Paeonia suffruticosa*. The AbA-containing SD/-Leu medium was used to screen the target genes for PsMYB44. (B) A dual-luciferase assay showed that PsMYB44 inhibited the transcription of *PsDFR* in tobacco leaves. Abbreviation: X, X-α-gal. The values are shown as the mean + SD, and different letters indicate significant differences ($P < 0.05$).

with an average of 834.4-fold of WT (Fig. 5B). Furthermore, *PsMYB44* transgenic flowers were subjected to measurement of colour indices, HPLC analysis and tobacco *DFR* gene expression analysis. As shown in Fig. 5C–E, the a^* value representing red colour was significantly lower in *PsMYB44* transgenic flowers compared with WT, and the anthocyanin accumulation also decreased by an average of 42.3 %. In addition, the tobacco *DFR* gene expression was repressed under exogenous overexpression of *PsMYB44*. Overall, these results demonstrated that PsMYB44 could negatively regulate anthocyanin biosynthesis by affecting *DFR* gene expression in plants.

Silencing PsMYB44 suppresses blotch formation in P. suffruticosa

Given that the genetic transformation system has not been established in *P. suffruticosa*, a TRV-based VIGS transient transformation assay was performed, and a TRV2-*PsMYB44* silencing vector was applied specifically to silence the mRNA level of *PsMYB44* in 'High noon'. After 7 days, PCR showed the successful transformation of *PsMYB44* in *P. suffruticosa* petals, and qRT-PCR was used to analyse the expression level of *PsMYB44*, which indicated that the *PsMYB44* transcription level was strongly silenced in *PsMYB44*-silenced petals, with a decrease of 88.9 % compared with WT (Supplementary Data Fig. S7). As shown in Fig. 6A, *PsMYB44*-silenced petals demonstrated darker blotch colour, and the red colour representing the a^* value was higher than that in WT, whereas the yellow colour representing the b^* value was much lower than that in WT (Fig. 6B). To investigate the reason for this, HPLC analysis was performed, and the red colour, representing total anthocyanin contents, and yellow colour, representing total anthoxanthin contents, were measured. We found that the total anthocyanin content increased by 16.1 % in *PsMYB44*-silenced petals, and the main anthocyanin component cyanidin-3,5-di-*O*-glucoside (Cy3G5G) made the main contribution, which increased by 29.1 % (Fig. 6C, D). Regarding anthoxanthins, the total anthoxanthin content of *PsMYB44*-silenced petals decreased by 12.3 % (Fig. 6E). Furthermore, the expression level of *PsDFR* was activated and increased 4.9-fold in *PsMYB44*-silenced petals compared with WT (Fig. 6F). Taken together, these results suggested that silencing *PsMYB44* activated *PsDFR* expression and redirected metabolic flux to anthocyanin biosynthesis, which promoted more anthocyanin accumulation in *P. suffruticosa* blotch areas.

DISCUSSION

The anthocyanin biosynthesis pathway and its related MYB regulators have been characterized widely in model woody and herbaceous plants and showed subtle variations among them (Stracke *et al.*, 2007; Yamagishi *et al.*, 2010; An *et al.*, 2019). To date, literature reports on transcriptional regulation of anthocyanin biosynthesis focus mainly on MBW positive regulators or MYB repressors represented by *Arabidopsis* AtMYB4 and

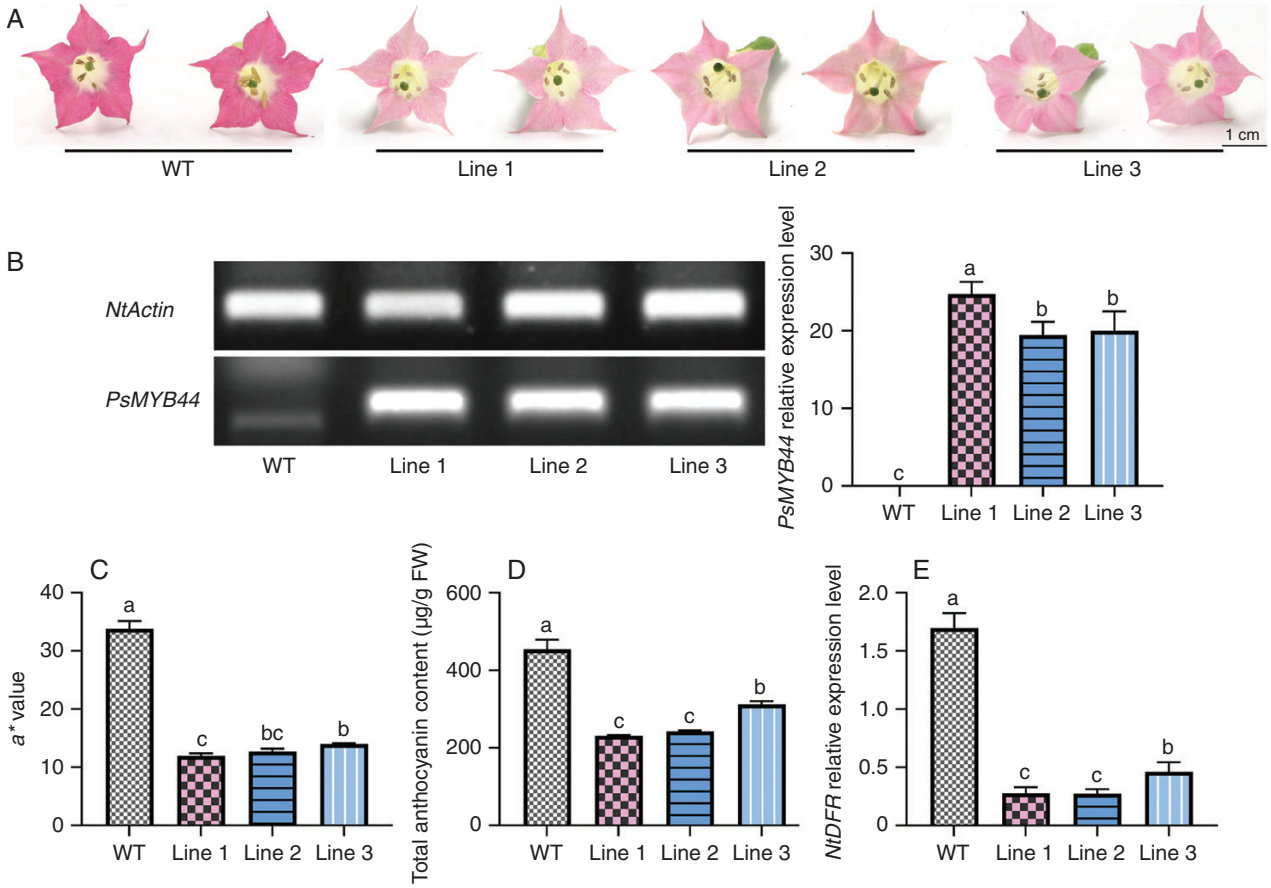

FIG. 5. *PsMYB44* functions as an anthocyanin repressor in tobacco flowers. (A) Changes in flower phenotype of wild-type (WT) and *PsMYB44* transgenic tobacco lines. (B) Expression analysis of *PsMYB44* in WT and *PsMYB44* transgenic tobacco lines validated by PCR and qRT-PCR. (C) Measurement of red representing *a** value in WT and *PsMYB44* transgenic tobacco lines. (D) Measurement of total anthocyanin content in WT and *PsMYB44* transgenic tobacco flowers. (E) Analysis of expression of *NtDFR* in WT and *PsMYB44* transgenic tobacco lines validated by PCR and qRT-PCR. The values are shown as the mean + SD, and different letters indicate significant differences ($P < 0.05$).

Fragaria × *ananassa* FaMYB1 (Aharoni *et al.*, 2001; Wang *et al.*, 2020; Chen *et al.*, 2022). Meanwhile, some atypical repressors have recently been identified in plants (An *et al.*, 2019; Wang *et al.*, 2022), and MYB44-like transcription factors are one of them. The MYB44-like transcription factors have been verified to participate in abiotic stress or the ABA response (Persak *et al.*, 2014; Kim *et al.*, 2017). To date, anthocyanin biosynthesis-related MYB44-like transcription factors have been identified in *S. tuberosum*, *I. batatas* and *Malus* crabapple (Liu *et al.*, 2019; Wei *et al.*, 2020; Li *et al.*, 2021*a*; Meng *et al.*, 2022), but the reports are still insufficient, and further investigation is required, especially regarding the regulation of flower colour and petal blotch formation. To study the potential regulatory mechanism of MYB44-like transcription factors on blotch formation in *P. suffruticosa*, in this study we searched for MYB44-like transcription factors based on *P. suffruticosa* transcriptome data. Eventually, one MYB44-like transcription factor, tentatively named PsMYB44, was found. Similar to other MYB44-like transcription factors in plants, PsMYB44 had a complete canonical repressive motif in its C-terminal, which has been verified as the embodiment of the repressor characteristic. In *S. tuberosum*, the repressive ability of StMYB44-2 was much lower than that of StMYB44-1 owing to one amino acid variation in the C2 motif, indicating that the sequence is crucial for its repressive ability (Liu *et al.*, 2019). In terms of phylogenetic relationships, PsMYB44 and MYB44-like transcription factors were clustered into a branch, and other members, such as *M. domestica* MdMYB6, *S. tuberosum* StMYB44-1 and StMYB44-2, have been reported to inhibit the biosynthesis of anthocyanin (Liu *et al.*, 2019; Xu *et al.*, 2020). Among these members, PsMYB44 shared 79 % homology with StMYB44-1, which reduced anthocyanin accumulation in *S. tuberosum* under high temperature stress (Liu *et al.*, 2019).

The spatial and temporal expression patterns of *PsMYB44* in 'High noon' petals at different developmental stages were revealed by qRT-PCR. The *PsMYB44* expression in the non-blotch areas was always higher than that in the blotch areas and reached the highest level in non-blotch areas at S4. It is worth noting that *PsMYB44* expression level increased gradually with blotch colour fading. These results indicated that *PsMYB44* was negatively correlated with blotch formation, both temporally and spatially. Petal blotches caused by spatially differential expression of transcription factors have been identified in *Clarkia gracilis* and *Mimulus* (Yuan *et al.*, 2014; Lin and Rausher, 2020). Three positive R2R3-MYB transcription factors (CgsMYB12, CgsMYB6 and CgsMYB11)

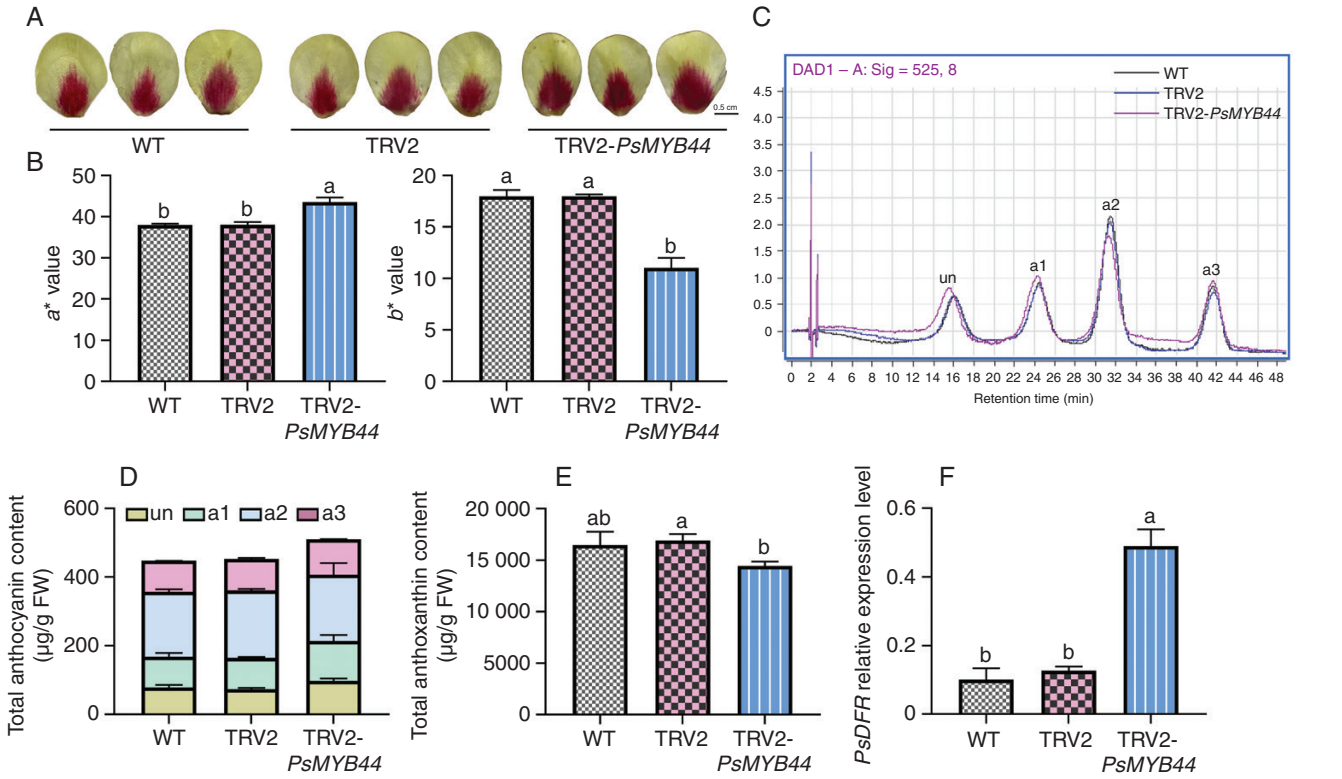

FIG. 6. Virus-induced gene silencing of *PsMYB44* in *Paeonia suffruticosa* petals. (A) Changes in flower phenotype of wild-type (WT), empty vector and *PsMYB44*-silenced petals. (B) Measurements of red representing *a** value and yellow representing *b** value in WT, empty vector and *PsMYB44*-silenced petals. (C) High-performance liquid chromatography analysis of anthocyanin in WT, empty vector and *PsMYB44*-silenced petals. Abbreviations: a1, Cy3G5G, cyanidin-3,5-di-*O*-glucoside; a2, Pn3G5G, peonidin-3,5-di-*O*-glucoside; a3, Cy3G, cyanidin-3-*O*-glucoside; and un, unidentified. (D) Quantitative analysis of total anthocyanins in WT, empty vector and *PsMYB44*-silenced petals. (E) Quantitative analysis of total anthoxanthins in WT, empty vector and *PsMYB44*-silenced petals. (F) Expression analysis of *PsDFR* in WT, empty vector and *PsMYB44*-silenced petals. The values are shown as the mean + SD, and different letters indicate significant differences ($P < 0.05$).

in *C. gracilis* and two positive R2R3-MYB transcription factors (MlPELAN and MlNEGAN) in *Mimulus* were differentially expressed in the different regions of the petals (Yuan *et al.*, 2014; Lin and Rausher, 2020), whereas negative R2R3-MYB transcription factors were rarely identified. Regarding MYB44-like transcription factors, *I. batatas IbMYB44.1-3* was highly expressed in the roots of orange or white sweetpotato cultivars but not red (Li *et al.*, 2021*a*). In *Malus* crabapple, *MrMYB44-like1–3* all showed opposite expression patterns to leaf anthocyanin content (Meng *et al.*, 2022). This meant that *MYB44s* might share a common negative regulatory function with them.

Given that *PsMYB44* is always negatively correlated with blotch formation and that multiple lines of evidence have shown that MYB proteins have impacts on anthocyanin-related target genes at the transcriptional level, the promoters of five structural genes were obtained and used in Y1H and dual-luciferase assays. The results showed that PsMYB44 could directly bind to the promoter of *PsDFR* in the yeast system and strongly suppress *PsDFR* promoter activity in *N. benthamiana* leaves. In *Freesia hybrida*, MYB repressors, such as FhMYB27 and FhMYBx, have been shown to participate in the anthocyanin feedback regulatory loop. The R2R3-MYB member FhMYB27 transformed the activated MBW complex to a repressive complex by interacting with FhTT8L, whereas R3-MYB member FhMYBx decreased anthocyanin accumulation by competing for the binding of FhPAP1 to FhTT8L (Li *et al.*, 2020). In *P. persica*, both the R3 domain located in the bHLH-binding site and the C1/2 motif in the C-terminal of PpMYB18 conferred repressive activity (Hui *et al.*, 2019). In our study, the bHLH-interacting motif was not found in the amino acid sequence of PsMYB44, and the Y2H assay also showed that PsMYB44 could not interact with PsbHLH1-3 proteins, indicating that PsMYB functioned as an anthocyanin repressor independent of the bHLH cofactors. In *S. tuberosum*, StMYB44-1 inhibited anthocyanin biosynthesis by suppressing expression level of *StDFR* (Liu *et al.*, 2019), and the same results were obtained here in *P. suffruticosa*. In *Arabidopsis*, the MYB SG22 family comprises AtMYB44, AtMYB70, AtMYB73 and AtMYB77, which are related to ethylene perception, signalling and response to abiotic stress (Liu *et al.*, 2011; Shim *et al.*, 2013; Bian *et al.*, 2020). To our knowledge, this is the first time that an MYB44-like member has been isolated in *P. suffruticosa*, and it was identified as a negative anthocyanin biosynthesis regulator in petals.

When tobacco heterologous transformation was introduced to study the function of *PsMYB44*, the *PsMYB44* transgenic tobacco flowers were significantly whitened, the total anthocyanin content was reduced by an average of 42.3 %, and the *PsDFR* homologous gene *NtDFR* in tobacco was also strongly

inhibited. Overexpression of *Malus* crabapple *MrMYB44-like1–3* in apples results in discoloured red peel, and similar results were obtained in red-skinned pears (Meng *et al.*, 2022). Furthermore, 'High noon' was used to verify the function of *PsMYB44*, and much redder blotch colours were observed in *PsMYB44*-silenced petals. Meanwhile, the total anthocyanin content accumulated more in blotch areas with a reduction in anthoxanthins, and this might be attributed to the activation of *PsDFR* in *PsMYB44*-silenced petals redirecting the metabolic flux of flavonoids to anthocyanin biosynthesis. Silencing *Malus* crabapple *MrMYB44-like* genes in transgenic leaf discs activated expression of *MrPAL*, *MrCHS*, *MrCHI*, *MrDFR* and *MrANS* to accumulate more anthocyanins (Meng *et al.*, 2022). Overall, few studies have focused on the role of *MYB44* in anthocyanin biosynthesis, and the specific mechanism of *PsMYB44* needs to be investigated further.

In this study, we demonstrated that the R2R3-MYB transcription factor PsMYB44 targeted the promoter of *PsDFR* and inhibited its expression in *P. suffruticosa* petals, which was a key factor in catalysing the conversion of dihydroqueretin to leucocyanidin. These findings not only revealed the regulatory effect of MYB44-like transcription factor on blotch formation but also laid a theoretical foundation for the study of the feedback regulation mechanism of anthocyanin biosynthesis in *P. suffruticosa*.

CONCLUSIONS

In conclusion, this work successfully isolated a new blotch formation-related transcription factor, PsMYB44, from *P. suffruticosa* petals. PsMYB44 belonged to the MYB SG22 family and have two typical repressive motifs. PsMYB44 was localized in the nucleus and showed significantly high expression in non-blotch areas, which was opposite to the spatial distribution of blotches. PsMYB44 negatively regulates blotch formation by targeting *PsDFR* promoter and inhibits its promoter activity, with an inhibition ratio of 60.0 %. Moreover, overexpression of *PsMYB44* reduced anthocyanin biosynthesis in tobacco flowers by 42.3 %, whereas silencing *PsMYB44* resulted in a darker blotch in *P. suffruticosa* petals. This study has revealed the molecular mechanism of the MYB44-like transcription factor in regulating petal blotch formation in *P. suffruticosa*, which provides a reference for the molecular breeding of blotched cultivars in the future.

SUPPLEMENTARY DATA

Supplementary data are available at *Annals of Botany* online and consist of the following.

Figure S1: overexpression of *PsMYB44* promoted by CaMV35S promoter for transient tobacco transformation.

Figure S2: yeast one-hybrid analysis verified by *PsMYB44* promoted by GAL4 promoter and candidate promoters driving an *AurR* gene.

Figure S3: yeast two-hybrid analysis between PsMYB44 and PsbHLH1-3.

Figure S4: overexpression of *PsMYB44* promoted by 2 × CaMV35S promoter for stable tobacco transformation.

Figure S5: silencing of *PsMYB44* promoted by CaMV35S promoter for *P. suffruticosa* petal transformation.

Figure S6: PsMYB44 could not interact with PsbHLH1-3 in the yeast system.

Figure S7: identification of VIGS of *PsMYB44* in *P. suffruticosa* petals.

Table S1: gene-specific primers used for gene and promoter isolation.

Table S2: gene-specific primers used for qRT-PCR detection in this study.

Table S3: gene-specific primers used for expression vector construction in yeast one-hybrid analysis.

Table S4: gene-specific primers used for expression vector construction in yeast two-hybrid analysis.

Table S5: gene-specific primers used for expression vector construction in dual-luciferase assays.

Table S6: gene-specific primers used for vector construction and transformed tobacco line identification.

Table S7: gene-specific primers used for vector construction and transformed *P. suffruticosa* line identification.

ACKNOWLEDGEMENTS

D.Z. and J.T. conceived and designed the project. Y.L., ZC. and Y.T. performed the experiments. Y.L., Z.C., Y.T., J.S., J.M., J.T. and D.Z. participated in discussions and contributed to the writing of the article.

FUNDING

This work was supported by the National Key R&D Program of China (grant number 2018YFD1000405), the Agricultural Science and Technology Independent Innovation Fund of Jiangsu Province (grant number CX(20)2030), Qing Lan Project of Jiangsu Province, Forestry Special Fund of Jiangsu Province, High-Level Talent Support Program of Yangzhou University, and Postgraduate Research & Practice Innovation Program of Jiangsu Province (grant number KYCX22_3521).

DATA ACCESSIBILITY STATEMENT

RNA-seq data from this study can be found in the GenBank data libraries under following accession number: SRP378683.

CONFLICT OF INTEREST

The authors declare no conflict of interest.

LITERATURE CITED

Aharoni A, **De Vos CHR**, **Wein M**, ***et al***. **2001**. The strawberry *FaMYB1* transcription factor suppresses anthocyanin and flavonol accumulation in transgenic tobacco. *Plant Journal* **28**: 319–332. doi:10.1046/j.1365-313x.2001.01154.x.

Albert NW, **Thrimawithana AH**, **McGhie TK**, ***et al***. **2018**. Genetic analysis of the liverwort *Marchantia polymorpha* reveals that R2R3-MYB activation of flavonoid production in response to abiotic stress is an ancient character in land plants. *New Phytologist* **218**: 554–566. doi:10.1111/nph.15002.

An JP, **Wang XF**, **Zhang XW**, ***et al***. **2019**. An apple MYB transcription factor regulates cold tolerance and anthocyanin accumulation and undergoes MIEL1-mediated degradation. *Plant Biotechnology Journal* **18**: 337–353. doi:10.1111/pbi.13201.

Anwar M, **Yu WJ**, **Yao H**, **Zhou P**, **Allan AC**, **Zeng LH. 2019**. *NtMYB3*, an R2R3-MYB from narcissus, regulates flavonoid biosynthesis. *International Journal Molecular Sciences* **20**: 5456.

Bian SM, **Jin DH**, **Sun GQ**, ***et al***. **2020**. Characterization of the soybean R2R3-MYB transcription factor *GmMYB81* and its functional roles under abiotic stresses. *Gene* **753**: 144803. doi:10.1016/j.gene.2020.144803.

Chen YZ, **Kim P**, **Kong LZ**, ***et al***. **2022**. A dual-function transcription factor, SlJAF13, promotes anthocyanin biosynthesis in tomato. *Journal of Experimental Botany* **73**: 5559–5580.

Du H, **Wu J**, **Ji KX**, ***et al***. **2015**. Methylation mediated by an anthocyanin, *O*-methyltransferase, is involved in purple flower coloration in *Paeonia*. *Journal of Experimental Botany* **66**: 6563–6577. doi:10.1093/jxb/erv365.

Eckhart VM, **Rushing NS**, **Hart GM**, **Hansen JD. 2006**. Frequency-dependent pollinator foraging in polymorphic *Clarkia xantiana* ssp. *xantiana* populations: implications for flower colour evolution and pollinator interactions. *Oikos* **112**: 412–421.

Gao JJ, **Shen XF**, **Zhang Z**, ***et al***. **2011**. The MYB transcription factor *MdMYB6* suppresses anthocyanin biosynthesis in transgenic *Arabidopsis*. *Plant Cell Tissue and Organ Culture* **106**: 235–242.

Glover BJ, **Walker RH**, **Moyroud E**, **Brockington SF. 2013**. How to spot a flower. *New Phytologist* **197**: 687–689. doi:10.1111/nph.12112.

Gu ZY, **Zhu J**, **Hao Q**, ***et al***. **2018**. A novel R2R3-MYB transcription factor contributes to petal blotch formation by regulating organ-specific expression of *PsCHS* in tree peony (*Paeonia suffruticosa*). *Plant Cell Physiology* **60**: 599–611.

Hellens RP, **Allan AC**, **Friel EN**, ***et al***. **2005**. Transient expression vectors for functional genomics, quantification of promoter activity and RNA silencing in plants. *Plant Methods* **1**: 13.

Hichri I, **Barrieu F**, **Bogs J**, **Kappel C**, **Delrot S**, **Lauvergeat V. 2011**. Recent advances in the transcriptional regulation of the flavonoid biosynthetic pathway. *Journal of Experimental Botany* **62**: 2465–2483. doi:10.1093/jxb/erq442.

Holton T, **Cornish E. 1995**. Genetics and biochemistry of anthocyanin biosynthesis. *Plant Cell* **7**: 1071–1083.

Huang D, **Wang X**, **Tang ZZ**, ***et al***. **2018**. Subfunctionalization of the *Ruby2–Ruby1* gene cluster during the domestication of citrus. *Nature Plants* **4**: 930–941. doi:10.1038/s41477-018-0287-6.

Hui Z, **Kui LW**, **Wang FR**, ***et al***. **2019**. Activator-type R2R3-MYB genes induce a repressor-type R2R3-MYB gene to balance anthocyanin and proanthocyanidin accumulation. *New Phytologist* **221**: 1919–1934.

Kim YY, **Cui MH**, **Noh MS**, **Jung KW**, **Shin JS. 2017**. The FBA motif-containing protein AFBA1 acts as a novel positive regulator of ABA response in Arabidopsis. *Plant and Cell Physiology* **58**: 574–586. doi:10.1093/pcp/pcx003.

Li CH, **Du H**, **Wang LS**, ***et al***. **2009**. Flavonoid composition and antioxidant activity of tree peony (*Paeonia* Section *Moutan*) yellow flowers. *Journal of Agricultural and Food Chemistry* **57**: 8496–8503. doi:10.1021/jf902103b.

Li LX, **Wei ZZ**, **Zhou ZL**, ***et al***. **2021***a*. A single amino acid mutant in the EAR motif of *IbMYB44.2* reduced the inhibition of anthocyanin accumulation in the purple-fleshed sweetpotato. *Plant Physiology and Biochemistry* **167**: 410–419. doi:10.1016/j.plaphy.2021.08.012.

Li P, **Feng D**, **Yang DC**, ***et al***. **2022**. Protective effects of anthocyanins on neurodegenerative diseases. *Trends in Food Science and Technology* **117**: 205–217.

Li X, **Li Y**, **Zhao MH**, ***et al***. **2021***b*. Molecular and metabolic insights into anthocyanin biosynthesis for leaf color change in chokecherry (*Padus virginiana*). *International Journal of Molecular Sciences* **22**: 10697.

Li YQ, **Shan XT**, **Gao RF**, ***et al***. **2020**. MYB repressors and MBW activation complex collaborate to fine-tune flower coloration in *Freesia hybrida*. *Communications Biology* **3**: 396.

Li YQ, **Shan XT**, **Tong LN**, ***et al***. **2021***c*. The conserved and particular roles of the R2R3-MYB regulator *FhPAP1* from *Freesia hybrida* in flower anthocyanin biosynthesis. *Plant Cell* **61**: 1365–1380.

Lin RC, **Rausher MD. 2020**. R2R3-MYB genes control petal pigmentation patterning in *Clarkia gracilis* ssp. *sonomensis* (Onagraceae). *New Phytologist* **229**: 1147–1162. doi:10.1111/nph.16908.

Liu RX, **Chen L**, **Jia ZH**, ***et al***. **2011**. Transcription factor *AtMYB44* regulates induced expression of the *ETHYLENE INSENSITIVE2* gene in *Arabidopsis* responding to a harpin protein. *Molecular Plant-Microbe Interactions* **24**: 377–389.

Liu YH, **Lin-Wang K**, **Espley RV**, ***et al***. **2019**. *StMYB44* negatively regulates anthocyanin biosynthesis at high temperatures in tuber flesh of potato. *Journal of Experimental Botany* **70**: 3809–3824. doi:10.1093/jxb/erz194.

Liu YL, **Schiff M**, **Marathe R**, **Dinesh-Kumar SP. 2002**. Tobacco *Rar1*, *EDS1* and *NPR1/NIM1* like genes are required for N-mediated resistance to tobacco mosaic virus. *Plant Journal* **30**: 415–429. doi:10.1046/j.1365-313x.2002.01297.x.

Luan YT, **Tang YH**, **Wang X**, **Xu C**, **Tao J**, **Zhao DQ. 2022**. Tree peony R2R3-MYB transcription factor PsMYB30 promotes petal blotch formation by activating the transcription of anthocyanin synthase gene. *Plant and Cell Physiology* **63**: 1101–1116. doi:10.1093/pcp/pcac085.

Lv SZ, **Cheng S**, **Wang ZY**, ***et al***. **2019**. Draft genome of the famous ornamental plant *Paeonia suffruticosa*. *Ecology and Evolution* **10**: 4518–4530.

Meng J-X, **Wei J**, **Chi R-F**, ***et al***. **2022**. MrMYB44-like negatively regulates anthocyanin biosynthesis and causes spring leaf color of *Malus* 'Radiant' to fade from red to green. *Frontiers in Plant Science* **13**: 822340.

Meng R, **Zhang J**, **An L**, ***et al***. **2016**. Expression profiling of several gene families involved in anthocyanin biosynthesis in apple (*Malus domestica* Borkh.) skin during fruit development. *Journal of Plant Growth Regulation* **35**: 449–464.

Miller R, **Owens SJ**, **Rorslett B. 2011**. Plants and colour: flowers and pollination. *Optics and Laser Technology* **43**: 282–294.

Moeller DA. 2005. Pollinator community structure and sources of spatial variation in plant–pollinator interactions in *Clarkia xantiana* ssp. *xantiana*. *Oecologia* **142**: 28–37.

Ni JB, **Premathilake AT**, **Gao YH**, ***et al***. **2021**. Ethylene-activated *PpERF105* induces the expression of the repressor-type R2R3-MYB gene *PpMYB140* to inhibit anthocyanin biosynthesis in red pear fruit. *Plant Journal* **105**: 167–181.

Persak H, **Pitzschke A. 2014**. Dominant repression by *Arabidopsis* transcription factor MYB44 causes oxidative damage and hypersensitivity to abiotic stress. *International Journal of Molecular Science* **15**: 2517–2537.

Petroni K, **Tonelli C. 2011**. Recent advances on the regulation of anthocyanin synthesis in reproductive organs. *Plant Science* **181**: 219–229. doi:10.1016/j.plantsci.2011.05.009.

Qi Y, **Zhou L**, **Han LL**, **Zou HZ**, **Miao K**, **Wang Y. 2020**. *PsbHLH1*, a novel transcription factor involved in regulating anthocyanin biosynthesis in tree peony (*Paeonia suffruticosa*). *Plant Physiology and Biochemistry* **154**: 396–408. doi:10.1016/j.plaphy.2020.06.015.

Rausher MD, **Miller RE**, **Tiffin P. 1999**. Patterns of evolutionary rate variation among genes of the anthocyanin biosynthetic pathway. *Molecular Biology and Evolution* **16**: 266–274. doi:10.1093/oxfordjournals.molbev.a026108.

Schaart JG, **Dubos C**, **De La Fuente IR**, ***et al***. **2013**. Identification and characterization of MYB-bHLH-WD40 regulatory complexes controlling proanthocyanidin biosynthesis in strawberry (*Fragaria* × *ananassa*) fruits. *New Phytologist* **197**: 454–467.

Shaner NC, **Campbell RE**, **Steinbach PA**, **Giepmans BNG**, **Palmer AE**, **Tsien RY. 2004**. Improved monomeric red, orange and yellow fluorescent proteins derived from *Discosoma* sp. red fluorescent protein. *Nature Biotechnology* **22**: 1567–1572. doi:10.1038/nbt1037.

Sheehan H, **Moser M**, **Klahre U**, ***et al***. **2016**. *MYB-FL* controls gain and loss of floral UV absorbance, a key trait affecting pollinator preference and reproductive isolation. *Nature Genetics* **48**: 159–166.

Shim JS, **Jung C**, **Lee S**, ***et al***. **2013**. YD *AtMYB44* regulates *WRKY70* expression and modulates antagonistic interaction between salicylic acid and jasmonic acid signaling. *Plant Journal* **73**: 483–495.

Song LY, **Wang XL**, **Han W**, ***et al***. **2020**. *PbMYB120* negatively regulates anthocyanin accumulation in pear. *International Journal of Molecular Sciences* **21**: 1528.

Stracke R, **Ishihara H**, **Barsch GHA**, **Mehrtens F**, **Niehaus K**, **Weisshaar B. 2007**. Differential regulation of closely related R2R3-MYB transcription factors controls flavonol accumulation in different parts of the *Arabidopsis thaliana* seedling. *Plant Journal* **50**: 660–677.

Sunilkumar G, **Vijayachandra K**, **Veluthambi K. 1999**. Preincubation of cut tobacco leaf explants promotes *Agrobacterium*-mediated transformation by increasing *vir* gene induction. *Plant Science* **141**: 51–58. doi:10.1016/s0168-9452(98)00228-3.

Tanaka Y, **Sasaki N**, **Ohmiya A. 2008**. Biosynthesis of plant pigments: anthocyanins, betalains and carotenoids. *Plant Journal* **54**: 733–749. doi:10.1111/j.1365-313x.2008.03447.x.

Tohge T, **Watanabe M**, **Hoefgen R**, **Fernie AR. 2013**. The evolution of phenylpropanoid metabolism in the green lineage. *Critical Reviews in Biochemistry and Molecular Biology* **48**: 123–152. doi:10.3109/10409238.2012.758083.

Tohge T, **de Souza LP**, **Fernie AR. 2017**. Current understanding of the pathways of flavonoid biosynthesis in model and crop plants. *Journal of Experimental Botany* **68**: 4013–4028. doi:10.1093/jxb/erx177.

Wang LH, **Tang W**, **Hu YW**, ***et al***. **2019***b*. A MYB/bHLH complex regulates tissue-specific anthocyanin biosynthesis in the inner pericarp of red-centered kiwifruit *Actinidia chinensis* cv. Hongyang. *Plant Journal* **99**: 359–378. doi:10.1111/tpj.14330.

Wang S, **Zhang Z**, **Li LX**, ***et al***. **2022**. Apple MdMYB306-like inhibits anthocyanin synthesis by directly interacting with MdMYB17 and MdbHLH33. *Plant Journal* **110**: 1021–1034. doi:10.1111/tpj.15720.

Wang XC, **Wu J**, **Guan ML**, **Zhao CH**, **Geng P**, **Zhao Q. 2020**. *Arabidopsis* MYB4 plays dual roles in flavonoid biosynthesis. *Plant Journal* **101**: 637–652.

Wang YC, **Sun JJ**, **Wang N**, ***et al***. **2019***a*. MdMYBL2 helps regulate cytokinin-induced anthocyanin biosynthesis in red-fleshed apple (*Malus sieversii* f. *niedzwetzkyana*) callus. *Functional Plant Biology* **46**: 187–196. doi:10.1071/fp17216.

Wei Z-Z, **Hu K-D**, **Zhao D-L**, ***et al***. **2020**. *MYB44* competitively inhibits the formation of the *MYB340-bHLH2-NAC56* complex to regulate anthocyanin biosynthesis in purple-fleshed sweet potato. *BMC Plant Biology* **20**: 258.

Xiang LL, **Liu XF**, **Li H**, ***et al***. **2019**. *CmMYB#7*, an R3 MYB transcription factor, acts as a negative regulator of anthocyanin biosynthesis in chrysanthemum. *Journal of Experimental Botany* **70**: 3111–3123. doi:10.1093/jxb/erz121.

Xu HF, **Zou Q**, **Yang GX**, ***et al***. **2020**. MdMYB6 regulates anthocyanin formation in apple both through direct inhibition of the biosynthesis pathway and through substrate removal. *Horticulture Research* **7**: 72.

Yamagishi M, **Shimoyamada Y**, **Nakatsuka T**, **Masuda K. 2010**. Two *R2R3-MYB* genes, homologs of Petunia *AN2*, regulate anthocyanin biosyntheses in flower tepals, tepal spots and leaves of Asiatic hybrid lily. *Plant and Cell Physiology* **51**: 463–474. doi:10.1093/pcp/pcq011.

Yuan YW, **Sagawa JM**, **Frost L**, **Vela JP**, **Bradshaw HD. 2014**. Transcriptional control of floral anthocyanin pigmentation in monkeyflowers (*Mimulus*). *New Phytologist* **204**: 1013–1027. doi:10.1111/nph.12968.

Zhang H, **Gong JX**, **Chen KL**, ***et al***. **2020***a*. A novel R3 MYB transcriptional repressor, MaMYBx, finely regulates anthocyanin biosynthesis in grape hyacinth. *Plant Science* **298**: 110588. doi:10.1016/j.plantsci.2020.110588.

Zhang XP, **Xu ZD**, **Yu XY**, ***et al***. **2019**. Identification of two novel R2R3-MYB transcription factors, *PsMYB114L* and *PsMYB12L*, related to anthocyanin biosynthesis in *Paeonia suffruticosa*. *International Journal of Molecular Sciences* **20**: 1055.

Zhang YZ, **Xu SZ**, **Cheng YW**, ***et al***. **2020***b*. Functional identification of *PsMYB57* involved in anthocyanin regulation of tree peony. *BMC Genetics* **21**: 124.

Zhang YZ, **Xu SZ**, **Ma HP**, ***et al***. **2021**. The R2R3-MYB gene *PsMYB58* positively regulates anthocyanin biosynthesis in tree peony flowers. *Plant Physiology and Biochemistry* **164**: 279–288. doi:10.1016/j.plaphy.2021.04.034.

Zhao DQ, **Tang WH**, **Hao ZJ**, **Tao J. 2015**. Identification of flavonoids and expression of flavonoid biosynthetic genes in two coloured tree peony flowers. *Biochemical and Biophysical Research Communications* **459**: 450–456. doi:10.1016/j.bbrc.2015.02.126.

Zhao DQ, **Luan YT**, **Shi WB**, **Zhang XY**, **Meng JS**, **Tao J. 2020**. A *Paeonia ostii* caffeoyl-CoA *O*-methyltransferase confers drought stress tolerance by promoting lignin synthesis and ROS scavenging. *Plant Science* **303**: 110765.